Supplementary Information

Fluorescence blinking in MoS_2 atomic layers by single photon energy transfer

Mai He[1], Cuihuan Ge[1], Kai Braun[3], Lanyu Huang[1], Xin Yang[2], Hepeng Zhao[1], Alfred J. Meixner[3], Xiao Wang[1], Anlian Pan[2*]*

[1]School of Physics and Electronics, Hunan University, Changsha 410082, China

[2]Key Laboratory for Micro-Nano Physics and Technology of Hunan Province, College of Materials Science and Engineering, Hunan University, Changsha 410082, China

[3]Institute of Physical and Theoretical Chemistry and LISA+, University of Tübingen, Auf der Morgenstelle 18, 72076, Tübingen, Germany

*Email: xiao_wang@hnu.edu.cn; anlian.pan@hnu.edu.cn

Table of Contents

Supplementary Note 1. Statistics of steady-state PL emission from QDs

Steady-state PL spectra from monodispersed QDs were recorded and the corresponding peak positions were collected. With the Gaussian fitting, we find that the distribution of the PL peak positions from about 120 QDs is approximately centered at 582.9 nm (Supplementary figure 1). These emission spectra of QDs overlap with the absorption spectrum of MoS_2, thus satisfying the prerequisite for FRET.

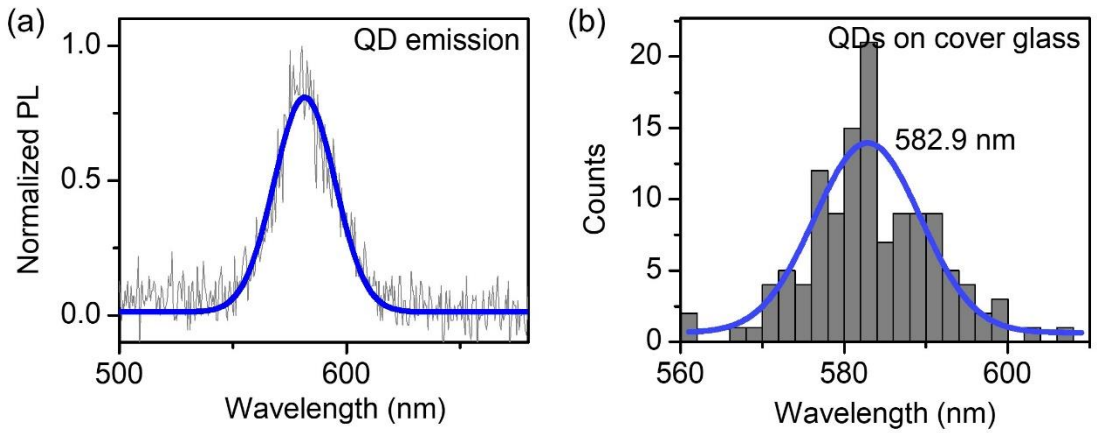

Supplementary figure 1. Steady-state PL of the monodispersed QDs. (a) Typical PL spectrum of a single QD at room temperature. (b) Statistics and the Gaussian fitting (sold blue line) of the PL emission peak distribution from 120 individual QDs.

Supplementary Note 2. Statistics of transient PL from QDs on cover glass and in heterostructures

To demonstrate the interaction between the QDs and the monolayer-MoS_2, fluorescence lifetime imaging (FLIM) of QDs and monolayer-MoS_2 in the heterostructure region were recorded (Supplementary figure 2b and 2c). Compared to that of QDs, the PL lifetime of MoS_2 is generally short. Furthermore, with FLIM (Supplementary figure 2c), PL decay curves (Supplementary figure 2d) and the statistics of PL lifetime (Supplementary figure 2e), we show that the PL lifetime of QDs in heterostructure (area of blue dashed lines) is much shorter than QDs on cover glass, which confirms the energy transfer between the QDs and the MoS_2 monolayer.

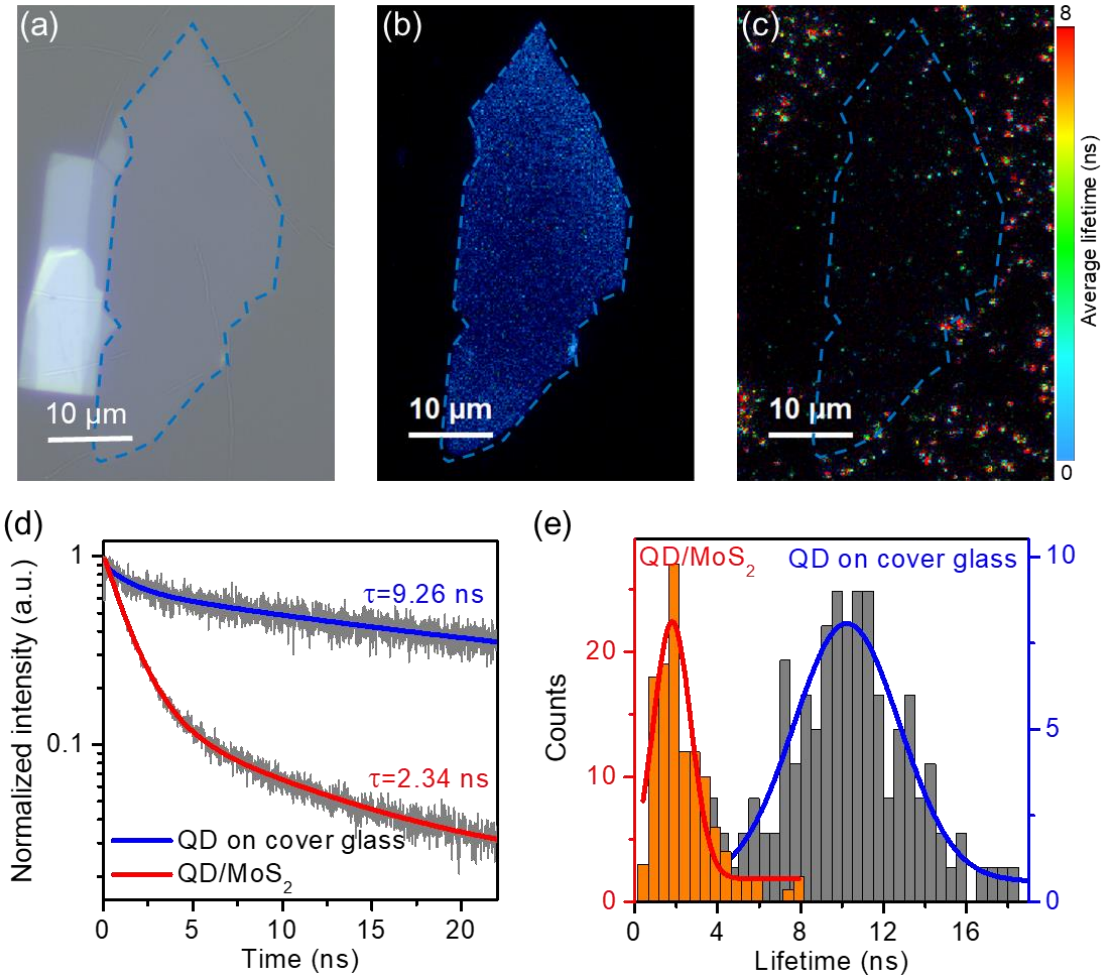

Supplementary figure 2. Fluorescence lifetime of QDs. (a) Optical image of a QD/MoS_2 heterostructure. (b), (c), Fluorescence Lifetime Imaging (FLIM) of MoS_2 and QDs in QD/monolayer-MoS_2 heterostructure. (d) Representative PL decay curves from QD on cover glass and in QD/MoS_2 heterostructure. (e) PL lifetime distributions and Gaussian fittings of QDs on cover glass (blue line) and in QD/monolayer-MoS_2 heterostructures (red line).

Supplementary Note 3. Fitting methods about second-order correlation function

For the second-order photon correlation data obtained using a cw excitation laser, the fitting model is adopted from the literature [1],

$$g^2(t) = 1 - (1+b) * \exp\left(\frac{-|t|}{\mathrm{tau}_1}\right) + b * \exp\left(\frac{-|t|}{\mathrm{tau}_2}\right) \quad (1)$$

Where tau_1 and tau_2 reflect the decay rates of the excited and metastable states, respectively, and b is a parameter in the fitting process. the $g^2(0)$ was extracted from the fitted curve at time $t = 0$. The fitting parameters of the second-order correlation function obtained under different conditions are shown in the following table, and the corresponding data are shown in Supplementary figure 3a.

The fitting parameters of the cw second-order correlation function

	b	tau_1(ns)	tau_2(ns)	$g^2(0)$
QD on cover glass	-0.18	39.4	0.44	0.18
QD covered by MoS_2	-0.45	16.8	0.01	0.45
QD covered by 2l-MoS_2	-0.23	28.3	0.11	0.23

While the pulsed second-order photon correlation data were fitted by the following formula [2], which is an n-peak fitting function.

$$D(t) = \sum_{0}^{n} (a + b_n * \exp(-|(t - t_n)/\mathrm{tau}_n|)) \quad (2)$$

where n is the peak number and a is a constant baseline; parameters b_n, t_n, tau_n are related to the height factor, center position and decay lifetime of the nth peak,

respectively. Once the fitting curve was obtained, the area of the *n*th peak was calculated by integral in the [t_n - 0.1, t_n + 0.1] region, namely,

$$A_n = \int_{t_n-0.1}^{t_n+0.1} (a + b_n * \exp(-|(t - t_n)/\mathrm{tau}_n|))dt \quad (3)$$

The $g^2(0)$ is defined as the ratio between the center peak area A_0 (or the area calculated from the peak with zero delay time) and the side peak average area A_{ave}. The fitting parameters of the second-order correlation function obtained under different conditions are shown in the following table, and the corresponding data are shown in Supplementary figure 3b.

The fitting parameters of the pulsed second-order correlation function

	a	b_{ave}	$\mathrm{tau}_{\mathrm{ave}}$(ns)	$g^2(0)$
QD on cover glass	0.393	2.91	31.23	0.05
QD covered by MoS_2	0.445	4.78	18.1	0.34
QD covered by 2l-MoS_2	0.388	3.69	24.11	0.16

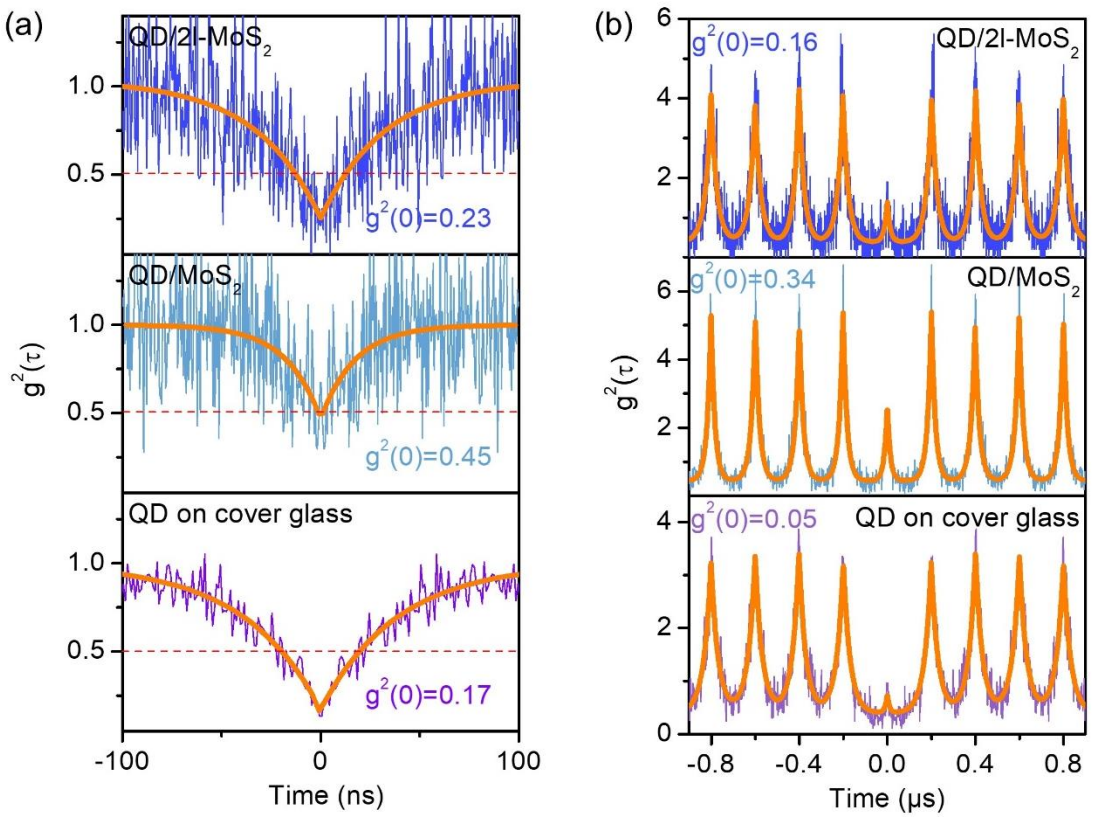

Supplementary figure 3. Single photon emission from QDs. (a), (b), The second-order photon correlation data from a QD on cover glass (lower panel), in QD/monolayer-MoS_2 heterostructure (middle panel) and in QD/bilayer-MoS_2 heterostructure (upper panel) excited by the cw and pulsed 405 nm laser. orange curves represent the corresponding fitting data using the above fitting methods.

Supplementary Note 4. Fluorescence correlation measurements in heterostructure

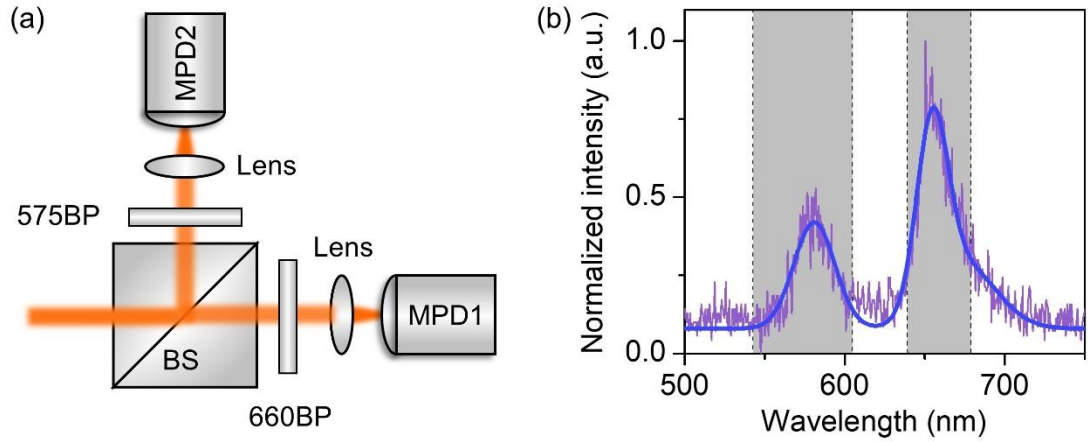

Supplementary figure 4. Experimental configuration for fluorescence correlation between MoS_2 and QD. (a) Schematic of fluorescence correlation experiments. The fluorescence signal is divided into two parts by a beam splitter, one of which passes through a 660 nm band-pass filter and is focused on the detector through a lens. The other beam passes through a 575 nm band-pass filter and is focused on another detector. In this way, the signals of MoS_2 and QD can be detected simultaneously. (b) PL spectrum of QD/monolayer-MoS_2 heterostructure. The blue curve is the fitting data of the spectrum (purple curve), and the gray areas represent the filtering range of these two filters.

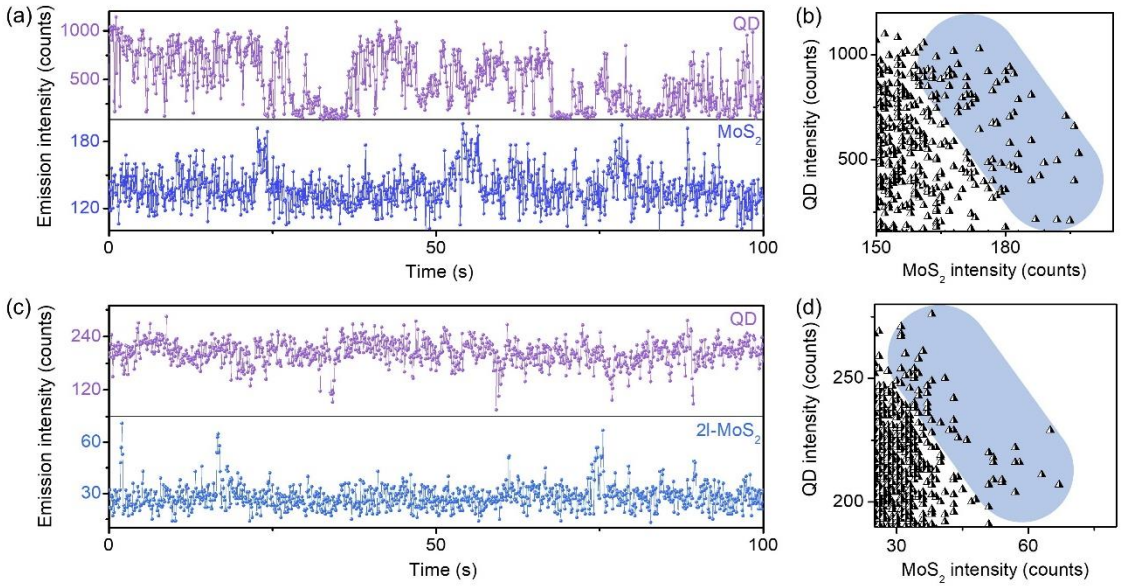

Supplementary figure 5. Fluorescence correlation from QD/monolayer-MoS_2 and QD/bilayer-MoS_2. (a) PL intensity time trajectories from QD (purple curve) and MoS_2 (blue curve) in QD/monolayer-MoS_2 heterostructure. (b) Emission intensity distribution of QD and MoS_2 from (a). These statistics reflect that a high emission intensity of MoS_2 is clearly associated with a low emission intensity of QD (blue area). (c) PL intensity time trajectories from the QD (purple curve) and bilayer-MoS_2 (blue curve) in QD/bilayer-MoS_2 heterostructure. A faint blinking is presented in bilayer-MoS_2 (2l-MoS_2). (d) The emission intensity distribution of QD and 2l-MoS_2 in (c).

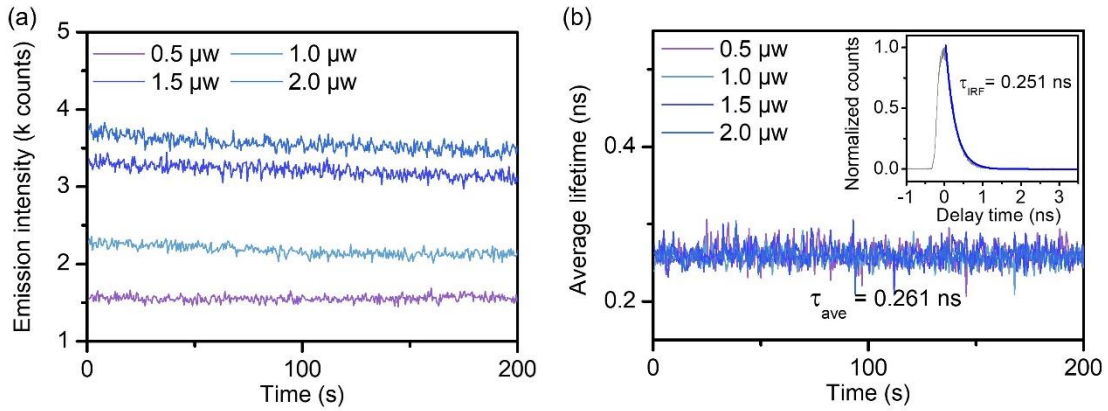

Supplementary figure 6. PL intensity and lifetime time trajectories from MoS_2 monolayer at different excitation powers. (a) PL time trajectories from MoS_2 at different excitation powers. The emission intensity of MoS_2 increases with the increase of excitation power and keeps relatively stable over time. (b) PL lifetime time trajectories at different excitation powers. The lifetime of MoS_2 was almost consistent at different excitation powers and remained relatively stable throughout the test period. The emission intensity in (a) and the fluorescence lifetime in (b) are extracted from the same fluorescence signal. The inset in (b) shows the instrument response function (IRF) of our system.

References

1. Tran, T. T., Bray, K., Ford, M. J., Toth, M. & Aharonovich, I. Quantum emission from hexagonal boron nitride monolayers. *Nat. Nanotechnol.* **11**, 37-41 (2016).
2. Li, C. *et al.* Purification of single-photon emission from hBN using post-processing treatments. *Nanophotonics* **8**, 2049-2055 (2019).